Supplemental material

Shima et al., https://doi.org/10.1083/jcb.201711178

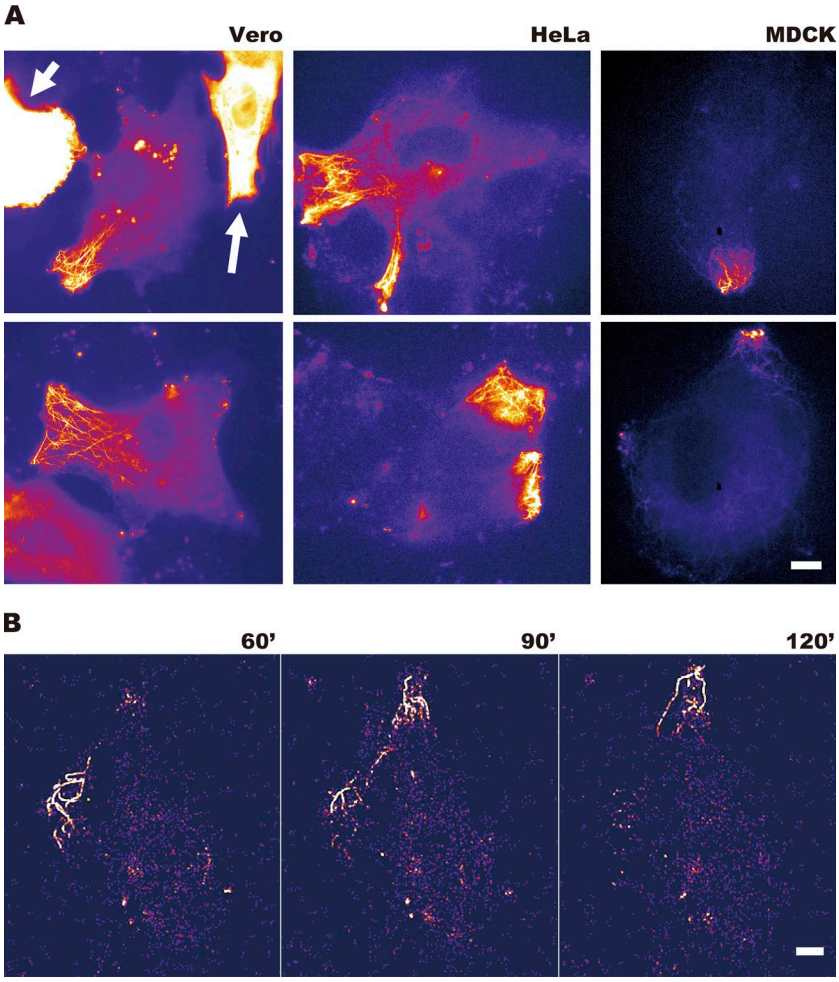

Figure S1. **Stochastic and transient asymmetric distribution of kinesin in nonneuronal cells. (A)** Asymmetric distribution of GFP-tagged KIF5C dimeric motor domain (aa 1–560) in various cells (Vero, MDCK, and HeLa). Only cells with low expression level of GFP-KIF5C were analyzed, so that the signals from the overexpressing cells are saturated in this presentation (arrows). Images are shown with pseudocolor ("Fire" lookup table of ImageJ) to illustrate the asymmetric distribution. Bar, 10 µm. **(B)** Total internal reflection fluorescence live-cell imaging of a HeLa cell expressing GFP-KIF5C. KIF5C asymmetrically distributes in the cell, and only a small subset of microtubules are heavily decorated with KIF5C. The accumulation of KIF5C, however, stochastically switches within ∼1 h. Pseudocolored SD maps at 60, 90, and 120 min are shown. Bar, 10 µm.

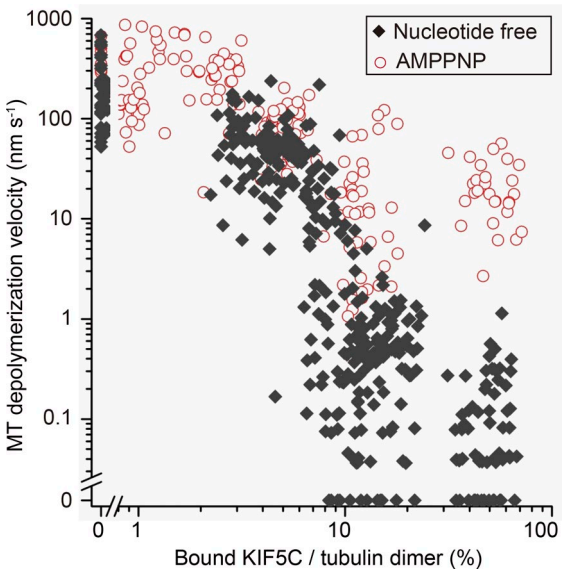

Figure S2. **Hyperstabilization of GDP microtubules by KIF5C.** KIF5C inhibited depolymerization of GDP microtubules (MT). The depolymerization velocity was sensitive to the nucleotide condition of KIF5C when more than 10% of the tubulin dimer was occupied by KIF5C. The number of KIF5C molecules bound on a microtubule was measured using the fluorescent intensity of KIF5C–DY647. See also Video 2.

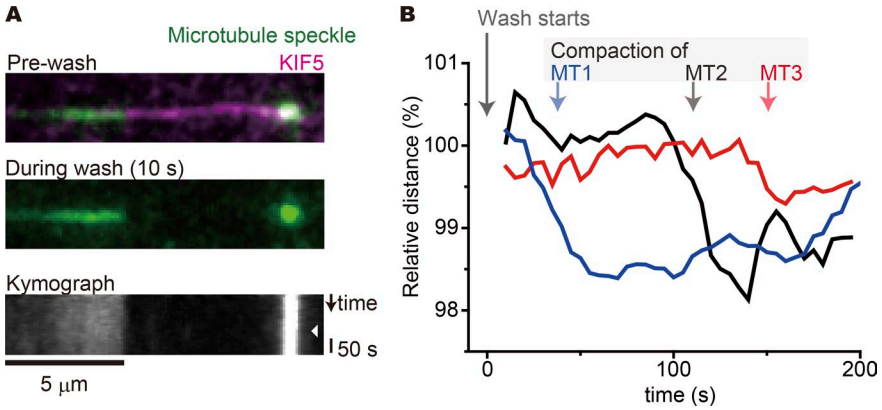

Figure S3. **Compaction of the elongated GDP microtubule. (A)** Images of fluorescent speckles on GDP microtubules (green) and KIF5C (magenta). Before the washout process, KIF5C bound throughout the microtubule (top panel), while KIF5C was washed out in less than 10 s of the washout process (middle panel). The bottom panel shows a kymograph of the speckles during the washout process. The distance between the speckles was shortened at 150 s after initiating the washout process (arrowhead). **(B)** The relative distances between the speckles after initiation of the KIF5C washout. The distances were shortened at 40–150 s, suggesting that GDP microtubules keep the KIF5C-induced elongated form for a while after KIF5C dissociation.

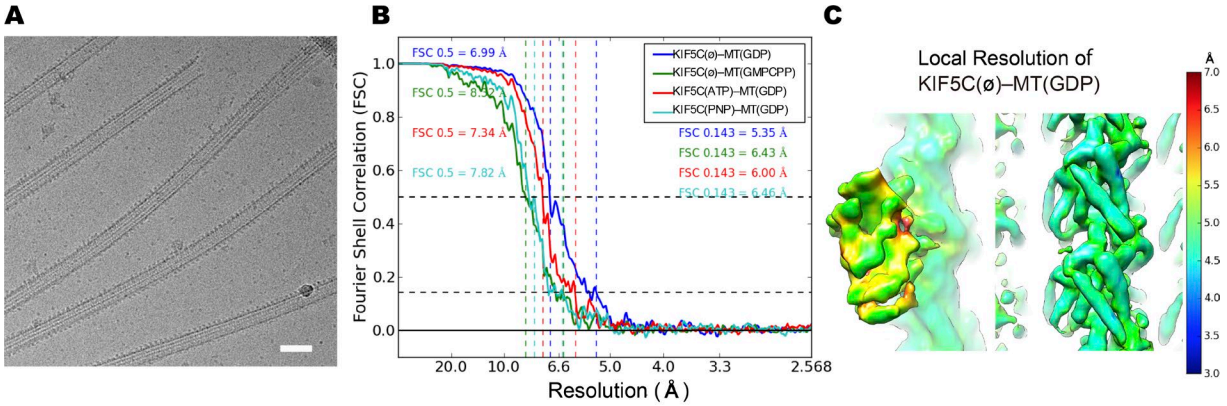

D

	Particle number	Resolution (Å) (FSC 0.143)	Mean Local Resolution (Å)	Median Local Resolution (Å)	3-start rise (Å)	3-start twist (°)	b-factor sharpening (Å^2)
KIF5C(PNP)–MT(GDP)	8507	6.46	4.82	4.75	8.6237	-25.768	120
KIF5C(ATP)–MT(GDP)	14302	6.00	4.65	4.5	8.70662	-25.7619	200
KIF5C(ø)–MT(GDP)	17173	5.35	4.64	4.5	8.70662	-25.7617	200
KIF5C(ø)–MT(GMPCPP)	5822	6.43	4.96	4.75	8.8632	-25.7541	200

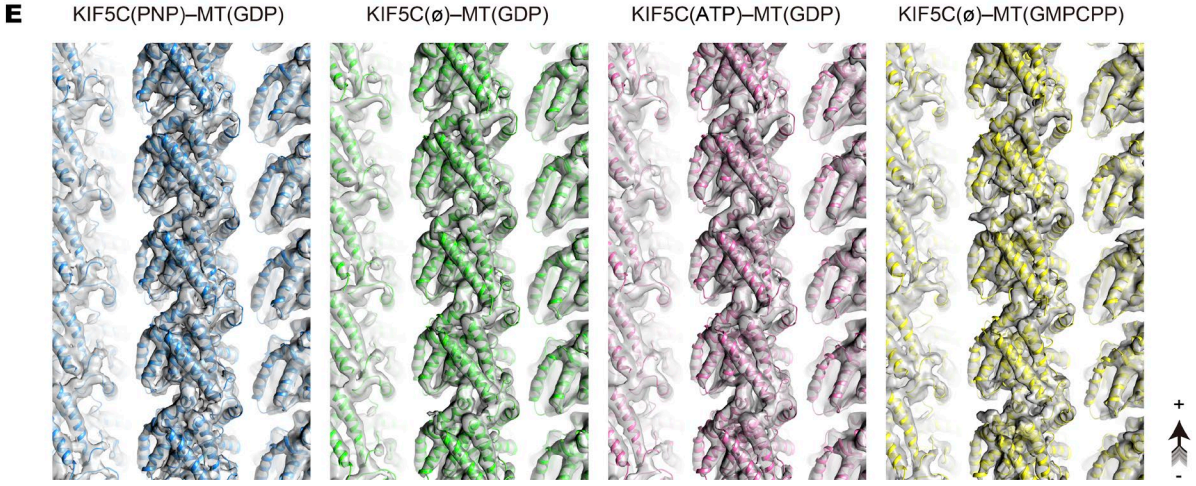

Figure S4. **Resolution and statistics for the cryo-EM reconstructions. (A)** Example micrograph of KIF5C(Ø)–MT(GDP). Bar, 50 nm. **(B)** Fourier shell correlation curves of the four KIF5C–MT reconstructions. **(C)** Example local resolution estimation of KIF5C(Ø)–MT(GDP) calculated by ResMap. **(D)** Image data processing statistics and helical parameters for the reconstructions. **(E)** The electron density maps and docked atomic models of the four KIF5C–MT complexes.

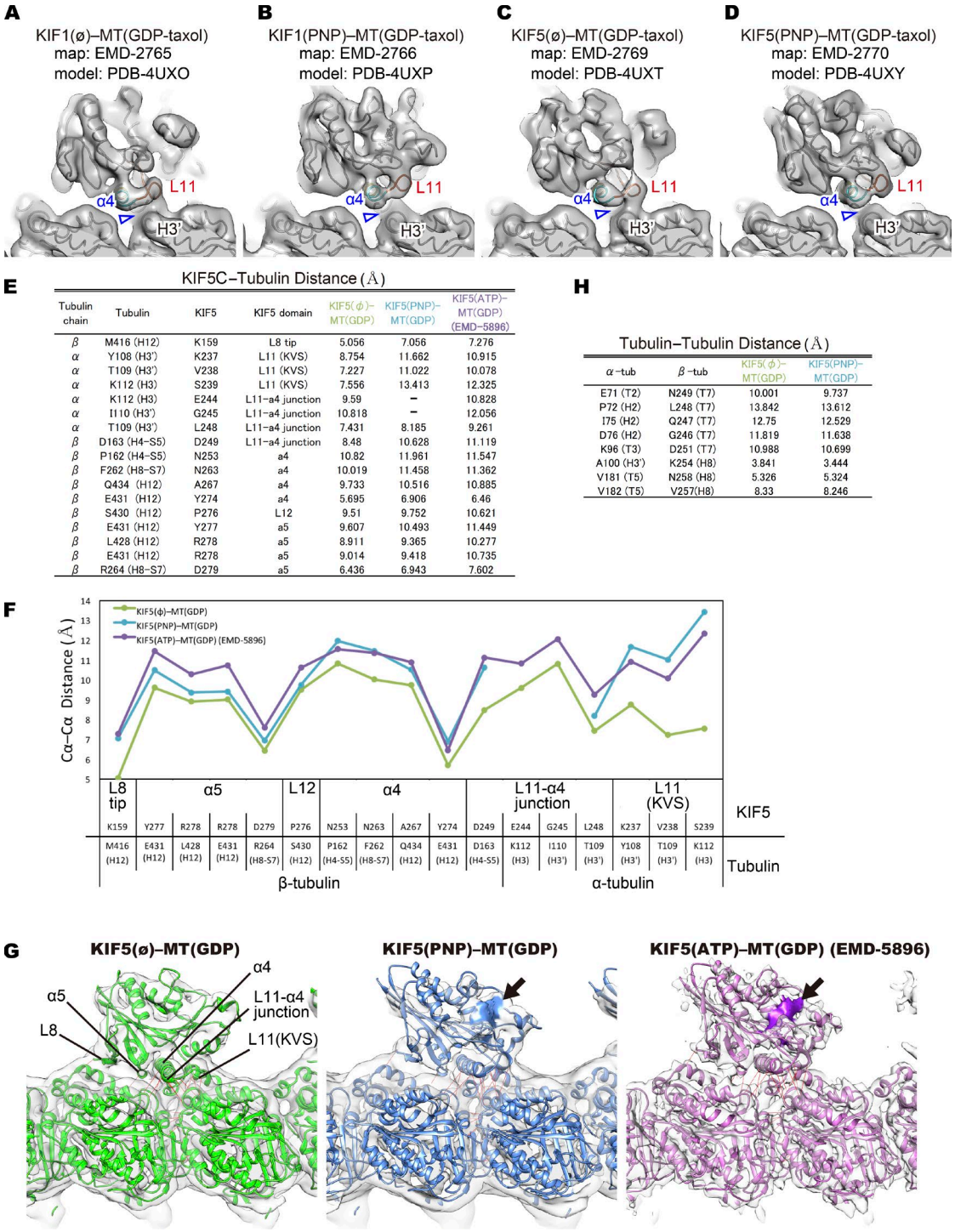

Tubulin chain	Tubulin	KIF5	KIF5 domain	KIF5(ϕ)–MT(GDP)	KIF5(PNP)–MT(GDP)	KIF5(ATP)–MT(GDP) (EMD-5896)
β	M416 (H12)	K159	L8 tip	5.056	7.056	7.276
α	Y108 (H3')	K237	L11 (KVS)	8.754	11.662	10.915
α	T109 (H3')	V238	L11 (KVS)	7.227	11.022	10.078
α	K112 (H3)	S239	L11 (KVS)	7.556	13.413	12.325
α	K112 (H3)	E244	L11–a4 junction	9.59	–	10.828
α	I110 (H3')	G245	L11–a4 junction	10.818	–	12.056
α	T109 (H3')	L248	L11–a4 junction	7.431	8.185	9.261
β	D163 (H4–S5)	D249	L11–a4 junction	8.48	10.628	11.119
β	P162 (H4–S5)	N253	a4	10.82	11.961	11.547
β	F262 (H8–S7)	N263	a4	10.019	11.458	11.362
β	Q434 (H12)	A267	a4	9.733	10.516	10.885
β	E431 (H12)	Y274	a4	5.695	6.906	6.46
β	S430 (H12)	P276	L12	9.51	9.752	10.621
β	E431 (H12)	Y277	a5	9.607	10.493	11.449
β	L428 (H12)	R278	a5	8.911	9.365	10.277
β	E431 (H12)	R278	a5	9.014	9.418	10.735
β	R264 (H8–S7)	D279	a5	6.436	6.943	7.602

α–tub	β–tub	KIF5(ϕ)–MT(GDP)	KIF5(PNP)–MT(GDP)
E71 (T2)	N249 (T7)	10.001	9.737
P72 (H2)	L248 (T7)	13.842	13.612
I75 (H2)	Q247 (T7)	12.75	12.529
D76 (H2)	G246 (T7)	11.819	11.638
K96 (T3)	D251 (T7)	10.988	10.699
A100 (H3')	K254 (H8)	3.841	3.444
V181 (T5)	N258 (H8)	5.326	5.324
V182 (T5)	V257(H8)	8.33	8.246

Figure S5. **Position of the elements of a kinesin–microtubule surface. (A–D)** The conformations of the L11-α4 junction of KIF1A (A and B) and KIF5C (C and D) reconstructed from the previous report (Atherton et al., 2014). The loop L11 and the following first turn of helix α4 do not change their conformations much with the nucleotide states in KIF1A (A and B). The L11-α4 junction region (cyan) is separate from the α-tubulin remarkably (arrowheads). The corresponding region of KIF5C takes a similar conformation on the GDP–Taxol microtubule (C and D). EMD, Electron Microscopy Data Bank; PDB, Protein Data Bank. **(E and F)** The Cα-Cα distances of KIF5 and tubulins in the KIF5(ø)–MT(GDP) and KIF5(PNP)–MT(GDP) structures reported here and the KIF5(ATP)–MT(GDP) (EMD-5896) structures previously reported by Alushin et al. (2014). For KIF5(ATP)–MT(GDP) docking, we rigidly fit 4HNA and 4LNU into KIF5 and microtubule densities, respectively. Comparing KIF5(ø)–MT(GDP) and KIF5(PNP)–MT(GDP), the tubulin and KIF5 interface elements (L8 tip, α5, L12, α4, L11-α4 junction, and L11 [KVS]) are closer in KIF5(ø)–MT(GDP) (green and blue lines in F), suggesting the interactions in KIF5(ø)–MT(GDP) are strong to rotate tubulins and elongate microtubules (MT). Those elements in KIF5(ATP)–MT(GDP) were similar to KIF5(PNP)–MT(GDP), especially in the L11 and α4 (purple and blue lines in F). **(G)** Side view of the three KIF5–MT complex structures for the distance measurements in E and F. KIF5(ATP)–MT(GDP) seems to contain a nucleotide (arrow) in the nucleotide-binding pocket. **(H)** The Cα-Cα distances for α- and β-tubulins in the KIF5(ø)–MT(GDP) and KIF5(PNP)–MT(GDP) structures.

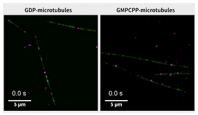

Video 1. **KIF5C dimer molecules (magenta) moving along GDP and GMPCPP microtubules (green).** Playback speed is 10×.

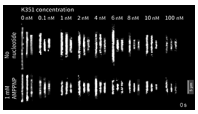

Video 2. **Depolymerization kinetics of GDP microtubules in the presence of KIF5C monomer (K351).** Three microtubule images are placed for each condition. Playback speed is 10×.

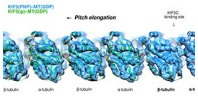

Video 3. **Comparison of the microtubule lattices between KIF5C(PNP)–MT(GDP) and KIF5C(ø)–MT(GDP).** Frame rate, 25 FPS.

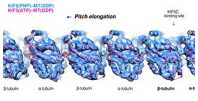

Video 4. **Comparison of the microtubule lattices between KIF5C(PNP)–MT(GDP) and KIF5C(ATP)–MT(GDP).** Frame rate, 25 FPS.

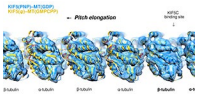

Video 5. **Comparison of the microtubule lattices between KIF5C(PNP)–MT(GDP) and KIF5C(ø)–MT(GMPCPP).** Frame rate, 25 FPS.

Table S1. **Sample and event numbers for Fig. 1 (G–L)**

Microtubule type	**GDP**			**GMPCPP**		
KIF5C (nM)	0.12	1.2	12	0.12	1.2	12
N_{MT}	83	65	61	60	56	54
N_{event}	37	119	252	40	82	125

Table S2. **Statistics for the mixed Gaussian fitting in Fig. 1 (G–I)**

		BIC			**First component**			**Second component**		
Microtubule type	**KIF5C (nM)**	**G = 1**	**G = 2**	**G = 3**	**λ**	**μ**	**σ**	**λ**	**μ**	**σ**
GDP	0.12	−321	−622[a]	−622	0.35	5×10^{-5}	3×10^{-5}	0.65	0.05	0.03
	1.2	−208	−260[a]	−252	0.46	0.01	0.008	0.54	0.09	0.05
	12	−217[a]	−213	NE	NA	0.09	0.04	NA	NA	NA
GMPCPP	0.12	−137[a]	−131	NE	NA	0.12	0.06	NA	NA	NA
	1.2	−182[a]	−181	−172	NA	0.09	0.04	NA	NA	NA
	12	−203[a]	−199	NE	NA	0.1	0.03	NA	NA	NA

BIC, Bayesian information criteria. λ, proportion; μ, mean; σ, SD of the Gaussian function. NE, not examined; NA, not applicable.
[a]The model with minimum Bayesian information criteria was chosen as the best fit.

Table S3. **Effects of increased KIF5C concentration on the motility-related parameters**

	GDP microtubule			GMPCPP microtubule		
	0.12 nM vs. 1.2 nM	**0.12 nM vs. 12 nM**	**1.2 nM vs. 12 nM**	**0.12 nM vs. 1.2 nM**	**0.12 nM vs. 12 nM**	**1.2 nM vs. 12 nM**
Landing rate (Fig. 1, G–I)	1.3 ± 0.1 (0.014)	3.2 ± 0.1 (8×10^{-11})	2.4 ± 0.2 (0.0013)	0.9 ± 0.4 (0.1)	1.0 ± 0.4 (0.47)	1.1 ± 0.3 (0.46)
Off rate (Fig. 1 J)	1.0 ± 0.1 (0.999)	1.0 ± 0.2 (0.85)	1.0 ± 0.2 (0.69)	1.3 ± 0.2 (5×10^{-5})	1.4 ± 0.4 (2×10^{-4})	1.0 ± 0.1 (0.93)
Velocity (Fig. 1 K)	1.1 ± 0.2 (0.004)	1.4 ± 0.1 (2×10^{-7})	1.2 ± 0.4 (5×10^{-9})	1.0 ± 0.2 (0.85)	1.2 ± 0.1 (0.50)	1.2 ± 0.1 (0.21)
Run length (Fig. 1 L)	1.0 ± 0.1 (0.35)	1.3 ± 0.1 (0.01)	1.2 ± 0.1 (0.07)	1.0 ± 0.2 (0.999)	0.9 ± 0.2 (0.99)	0.9 ± 0.2 (0.96)

Results of multiple comparisons by Steel–Dwass test are presented as a ratio of the median values ± SEM (P value).

Table S4. **Number of microtubules and kinesin observed for Fig. 2**

	Wild-type KIF5C		**Wild-type KIF5C**		**Wild-type KIF5C**	**L11 mutant KIF5C**	
	Nucleotide-free		**1 mM AMPPNP**		**Nucleotide-free**	**Nucleotide-free**	
KIF5C (M)	**GDP**	**GMPCPP**	**GDP**	**GMPCPP**	**Taxol**	**GDP**	**GMPCPP**
10^{-12}	170 (4)	57 (5)	NE	NE	217 (0)	24 (2)	19 (2)
10^{-11}	308 (15)	128 (47)	62 (3)	62 (4)	116 (30)	32 (5)	20 (4)
10^{-10}	144 (212)	53 (137)	62 (11)	61 (8)	98 (49)	28 (40)	30 (46)
10^{-9}	223 (3,687)	65 (1266)	105 (172)	60 (91)	121 (422)	29 (398)	26 (355)
10^{-8}	160 (28,341)	124 (14,026)	57 (347)	71 (768)	154 (837)	38 (8,370)	18 (4,522)
10^{-7}	NE	NE	55 (1,200)	59 (958)	NE	NE	NE

The data are represented as the number of microtubules (the number of bound KIF5C molecules). NE, not examined.

Table S5. **Statistics for the mixed Gaussian fitting in Fig. 2 B**

		BIC			**First component**			**Second component**		
Microtubule type	**KIF5C**	**G = 1**	**G = 2**	**G = 3**	**λ**	**μ**	**σ**	**λ**	**μ**	**σ**
GDP	10 pM	−253	−2073[a]	−2130	0.42	5×10^{-5}	3×10^{-5}	0.58	0.23	0.14
	100 pM	250	223[a]	234	0.17	0.10	0.06	0.83	1.03	0.47
GMPCPP	10 pM	−82.6[a]	−82.6	−74.4	NA	0.30	0.17	NA	NA	NA
	100 pM	129[a]	136	NE	NA	1.69	0.76	NA	NA	NA

BIC, Bayesian information criteria. NE, not examined; NA, not applicable.
[a]The model with minimum Bayesian information criteria was chosen as the best fit.

Table S6. **Statistics for the mixed Gaussian fitting in Fig. 2 D**

		BIC			First component			Second component		
Microtubule type	**KIF5C**	**G = 1**	**G = 2**	**G = 3**	**λ**	**μ**	**σ**	**λ**	**μ**	**σ**
GDP	100 pM	−211[a]	−203	NE	NA	0.174	0.03	NA	NA	NA
	1 nM	35	12[a]	22	0.7	0.52	0.016	0.3	0.96	0.28
GMPCPP	100 pM	−129[a]	−129	−124	NA	0.2	0.07	NA	NA	NA
	1 nM	11[a]	16	NE	NA	0.56	0.25	NA	NA	NA

BIC, Bayesian information criteria. NE, not examined; NA, not applicable.
[a]The model with minimum Bayesian information criteria was chosen as the best fit.

References

Alushin, G.M., G.C. Lander, E.H. Kellogg, R. Zhang, D. Baker, and E. Nogales. 2014. High-resolution microtubule structures reveal the structural transitions in αβ-tubulin upon GTP hydrolysis. *Cell.* 157:1117–1129. https://doi.org/10.1016/j.cell.2014.03.053

Atherton, J., I. Farabella, I.M. Yu, S.S. Rosenfeld, A. Houdusse, M. Topf, and C.A. Moores. 2014. Conserved mechanisms of microtubule-stimulated ADP release, ATP binding, and force generation in transport kinesins. *eLife.* 3:e03680. https://doi.org/10.7554/eLife.03680